Available online at www.sciencedirect.com
SCIENCE DIRECT®
Journal of Molecular Catalysis A: Chemical 240 (2005) 109–118
JOURNAL OF MOLECULAR CATALYSIS A: CHEMICAL
www.elsevier.com/locate/molcata

Phosphomolybdic acid supported on silica gel and promoted with alkali metal ions as catalysts for the esterification of acetic acid by ethanol

M.M.M. Abd El-Wahab *, A.A. Said

Chemistry Department, Faculty of Science, Assiut University, Assiut 71516, Egypt

Received 12 September 2004; received in revised form 5 May 2005; accepted 22 June 2005
Available online 2 August 2005

Abstract

Different ratios of phosphomolybdic acid PMA supported on silica gel (1–30 wt%) and promoted with alkali metal hydroxide have been prepared by an impregnation method and calcinated at 350 °C for 4 h. The catalysts were characterized by thermogravimetry (TG), differential thermal analysis (DTA), X-ray diffraction, FT-IR spectroscopy and N_2 adsorption measurements. The surface acidity and basicity of the catalysts were determined by adsorption of pyridine and the dehydration–dehydrogenation of 2-propanol. The gas-phase esterification of acetic acid by ethanol was carried out in a conventional flow bed reactor. The results clearly revealed that among the PMA loading, the use of 10 wt% catalyst showed maximum yield of ethyl acetate. This catalyst also improved on addition of Na or K-hydroxide. These results were correlated with the structure and the acid–base properties of the prepared catalysts.

Keywords: Esterification; Acetic acid; Ethanol; Silica-supported phosphomolybdic acid; Alkali metal dopants

1. Introduction

Heteropoly acids HPAs have stimulated considerable research in both heterogeneous and homogeneous catalysis [1–6]. Due to their bifunctional character, HPA catalysts are appropriate catalysts for both acid-catalyzed and redox reactions. The importance and full characterization of various HPAs and their properties, as commercially available catalysts, have been reviewed in the literature [6–9]. Solutions of these materials exhibit very strong Brönsted acidity with acid strengths higher than that of typical mineral acids [10,11]. In addition, their application in polar solvents poses the same problems as other liquid acid catalysts. However, chemical processes using such highly soluble acid catalyst require a catalyst separation process after reaction, due to the high toxicity and corrosiveness of the catalysts. These processes not only consume a large amount of energy, but also generate a large amount of chemical wastes. Therefore, many researchers have made efforts to develop such solid catalysts [12–15]. The use of insoluble solids HPAs as catalytic materials in liquid-phase reactions as replacement for homogeneous catalysts has recently been a major goal in catalysis research. Easy recovery without necessity of aqueous treatment during work-up procedures, and possibility of regeneration are the main advantages of the application of heterogeneous catalysts. On the other hand, the main disadvantage is their very low surface area. Thus, the use of support [1,15] allowing the HPA to be disappeared over a large surface area must result in an increase of its catalytic activity. The chemical interactions between the HPA and the support are a matter of great interest because a strong interaction could fix the HPA to the carrier, avoiding the leaching of HPA in liquid-phase reactions or maintaining a high HPA dispersion in gas-phase reactions [15,16]. Therefore, to avoid the strong solvation of acid sites with polar solvent and leveling their acid strength, the gas-phase esterification reaction is an important method to achieve this reaction. The main advantages of this method are the possibility of regeneration of the catalysts and reduction of the environmental impact. Recently [17–19], we have got good results on the gas phase esterification of acetic acid with ethyl alcohol using various heterogeneous catalytic

* Corresponding author. Tel.: +20 88 2411469; fax: +20 88 2342708.
E-mail address: wahabm@acc.aun.edu.eg (M.M.M. Abd El-Wahab).

1381-1169/$ – see front matter © 2005 Elsevier B.V. All rights reserved.
doi:10.1016/j.molcata.2005.06.038

systems. However, the catalytic gas phase esterification of acetic acid with ethyl alcohol on phosphomolybdic acid supported on silica system and treated with alkali metal ions to our knowledge, has not been reported. The purpose of this study was to examine the catalytic activity and selectivity of phosphomolybdic acid supported on silica gel and modified with alkali metal hydroxides towards the gas-phase esterification of acetic acid by ethyl alcohol. Particularly, the structure and surface properties of the prepared catalysts were investigated.

2. Experimental

2.1. Materials

Acetic acid, ethyl alcohol, isopropyl alcohol and pyridine were pure reagents and were used without further purification. Silica gel (grade, 60–200 mesh), the support material and phosphomolybdic acid were Merck and alkali metal hydroxides were commercially suppliers. The catalysts were prepared by impregnation of silica gel with various loading of phosphomolybdic acid (PMA) dissolved in doubly distilled water. The samples produced were dried in an oven at 100 °C for 24 h before being calcined at 350 °C for 4 h in a static air atmosphere. The content of PMA added varied between 1 and 30 wt% (silica induced PMA denoted by PMAS). The original catalyst containing 10 wt% PMA (PMASl0) treated with solutions containing known amounts of alkali metal hydroxides and dried at 100 °C for 24 h before being precalcined at 350 °C for 4 h. The contents of Li, Na or K-hydroxides were 1, 3 and 5 wt%.

2.2. Apparatus and techniques

2.2.1. Thermal analysis

Thermogravimetry (TG) and differential thermal analysis (DTA) were performed on heating (at 10 °C min^{-1}) test samples up to 600 °C in a dynamic atmosphere of air (40 ml min^{-1}), whereas the samples treated with pyridine (PY), the heating rate was 20 °C min^{-1} and flowing of 40 ml min^{-1} of N_2 using Computerized Shimadzu Thermal Analyzer TA60 Apparatus (Japan).

2.2.2. FT-IR spectroscopy

FT-IR spectra of the prepared catalysts calcined at 350 °C for 4 h were recorded in the 2000–200 cm^{-1} region with a Nicolet 710 FT-IR equipped with data station. Dried samples of 20 mg each were mixed with 100 mg of dry KBr and pressed into a disk.

2.2.3. X-ray diffraction (XRD)

XRD of the test samples was performed with a Philips diffractometer (Model PW 2103, $\lambda = 1.5418$ Å, 35 kV and 20 mA) with a source of Cu Kα radiation (Ni filtered). An on-line data acquisition and handling system facilitated automatic JCPDS library search and match for phase identification purposes.

2.2.4. Nitrogen gas adsorption

Nitrogen gas adsorption–desorption isotherms were measured at −196 °C using Nova 3200 instrument (Quantachrom Instrument Corporation, USA). Test samples were thoroughly outgassed for 2 h at 200 °C. The specific surface area, S_{BET}, was calculated applying the BET equation.

2.2.5. Acidity and basicity determination

The acidity and basicity of the catalysts under investigation were determined by the adsorption of pyridine and the dehydration–dehydrogenation of isopropyl alcohol (IPA) using procedures similar to that used in the catalytic activity measurements, except nitrogen was used as a carrier gas. The adsorption of pyridine was monitored by FT-IR spectroscopy [6] and the surface acid sites density was estimated by TG analysis as described elsewhere [20,21].

2.2.6. Catalytic activity measurements

The catalytic activity of the catalysts for the vapor-phase esterification of acetic acid with ethyl alcohol was carried out at 225 °C in a conventional fixed-bed flow type reactor at atmospheric pressure using dry air as a carrier gas. The system compressed two reactors, one of them was used without any catalyst and filled with glass beads (control reactor), enabled a measurement of the blank conversion (if occurred) which was subtracted from measured with flow reactor. A 0.5 g catalyst was placed in the middle of the reactor with quartz wool. Space in the reactor pre- and post-heating zone was filled with glass beads to reduce the effect of auto-oxidation of the substrate and products in the gas phase. The mixture of ethanol, acetic acid and air was introduced into the reactor after air bubbled through ethyl alcohol and acetic acid saturators. The total flow rate was fixed at 130 ml min^{-1} and using 1.6 and 2.1% ethanol and acetic acid in the gas feed, respectively. The gases after reaction were chromatographically analyzed by a FID on a Unicam ProGC using 2 m DNP and 10% PEG400 glass columns for the analysis of the reaction products of ethanol, acetic acid and isopropanol on the tested catalysts. The measurements of the conversion and yield (in %) were recorded after 2 h from the initial introduction of the reactants into the reactor to ensure the attainment of the reaction equilibrium (steady-state conditions).

3. Results and discussion

3.1. Thermal analysis

Fig. 1 represents the TG and DTA curves of the pure Silica, pure PMA and supported on silica. It shows that silica precursor loses weight with heating from room temperature up to 600 °C. However, nearly 70% of this loss occurred below 150 °C. This weight loss, which is accompanied by a broad

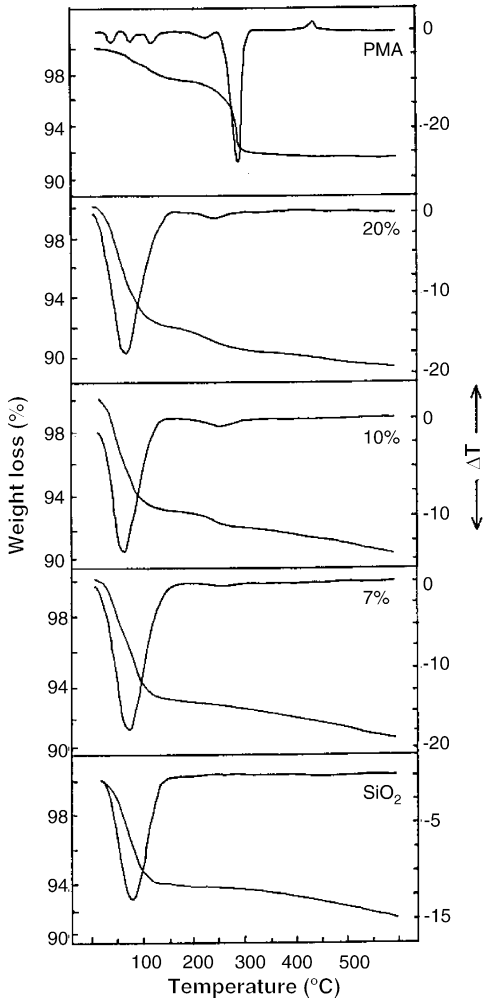

Fig. 1. TG and DTA curves of PMA supported on silica.

band peaking at 80 °C, can be attributed to vaporization of physically adsorbed water. Above 150 °C and up to 600 °C gradual weight loss was observed. The weight loss in this region can be considered as a result of dehydroxylation of hydroxyl groups. Unsupported PMA, shows that the weight loss exhibits six peaks on heating up to 600 °C maximized at 50, 87, 129, 232, 294 and 438 °C as indicated by the DTA curve. This behavior reflects that PMA loses its water of crystallization on heating up to 300 °C to give Keggin structure. The peak observed on DTA curve at 430 °C may correspond to the decomposition of Keggin unit of PMA [22,23] to give MoO_3. Curves for 7, 10 and 20 wt% PMA supported on silica show that the weight loss observed on heating up to 100 °C corresponds to physisorbed water. The broad peaks observed on the DTA curves between 150 and 300 °C may be attributed to the dehydroxylation of chemisorbed water and the water molecules adsorbed strongly retained [24] in the porous silica network. It is observed that, the loss of water of the supported acid a distinct shifted towards higher temperatures. This phenomenon clearly indicates thermal stabilization of the acid layer deposited within the silica pores [23]. Further heating up to 600 °C, a continuous weight loss observed on the TG curves.

3.2. FT-IR Spectra

Fig. 2a represents the FT-IR transmission spectra of pure SiO_2 and supported PMA catalysts calcined at 350 °C for 4 h. It shows a typical infrared spectrum of silica [25,26] with bands assigned at 1640, 970 and 800 cm^{-1} together with a broad band at 1100 cm^{-1}. The spectrum of pure PMA shows four bands in the range 1250–500 cm^{-1}. These bands are assigned at 1070, 1000, 878 and 790 cm^{-1}, which are the characteristic bands of the Keggin structure. These were assigned [26–29] to ν_{as}(P–O_a), ν_{as}(Mo–O_a), ν_{as}(Mo–O–Mo) and ν_{as}(Mo–O_c–Mo), respectively. In addition, the observed band at 595 cm^{-1} may be attributed to the δ(P–O) vibration [30]. Moreover, the band located at 1635 cm^{-1} may be characteristic the O–H stretching vibration. The FT-IR spectra of the different loading of PMA into silica indicate that most of characteristic bands of the parent Keggin structure, could be found in PMA fingerprint region (1250–500 cm^{-1}), are not shown or appeared in the same assignable position of the bands correspond to SiO_2 host material. It is reasonable to mention here that the band assigned at 1000 cm^{-1} in spectrum of pure PMA is shifted to lower vibration band, at 965 cm^{-1}. This means that some interaction effect may occur between PMA and SiO_2 support. Moreover, the small band assigned at 878 cm^{-1}, which characteristic ν_{as} (Mo–O–Mo), appear in the spectra of the samples containing 10, 20 and 30 wt% PMA.

Fig. 2b–d represents the FT-IR spectra of PMAS10 catalyst doped with 1, 3 and 5 wt% Li, Na or K-hydroxides and precalcined at 350 °C for 4 h. It can be seen from these curves that: (i) the treatment of PMAS10 with LiOH resulted in an increase in the intensity of the transmission band assigned at 1630 cm^{-1} indicating an increase in the concentration of OH group. On the other hand, a progressive decrease in the intensity of the bands assigned at 965 and 878 cm^{-1} indicates an effective change in the Keggin structure and (ii) doping of PMAS10 catalyst with NaOH or KOH shows a slight effect on the intensity of the bands belong to OH groups and that corresponds to the Keggin structure.

3.3. X-ray diffraction

X-ray diffraction of pure PMA and supported on silica gel samples calcined at 350 °C was carried out. The diffractograms of SiO_2 mixed with different contents of PMA are shown in Fig. 3. It shows a typical characteristic reflections of the Keggin structure of pure PMA whereas the sample containing 30 wt% PMA shows some reflections of PMA can be seen above 25° (2θ). On the other hand, the samples containing 3, 5 or 10 wt% PMA, curves show that the characteristic reflections of PMA disappeared and only a broad band centered around 2θ = 22° appears amorphous silica. The same phenomenon occurs by the inclusion of phosphotunges-

tic acid in silica [31] and also observed by impregnating HPAs onto MCM-41 due to the high surface area of these support materials [4,32].

The information acquired by IR, XRD, TG and DTA suggests a strong interaction between the host silica network and the guest PMA molecules. It follows that PMA in the silica include samples prepared here are finally dispersed and strongly bound in the porous silica network. These observations are in accordance with earlier findings indicating the reliability of the preparation method [2,33,34].

3.4. Surface area and porosity

The surface area and porosity of PMA supported on silica gel samples calcined at 350 °C were determined on the basis of nitrogen adsorption and desorption measurements. The isotherms show a type II of BDDT classification [35] with closed hysteresis loops at intermediate relative pressure. The pore size distribution for these samples could be determined from the desorption data. The specific surface area of the investigated catalysts, S_{BET} and the pore

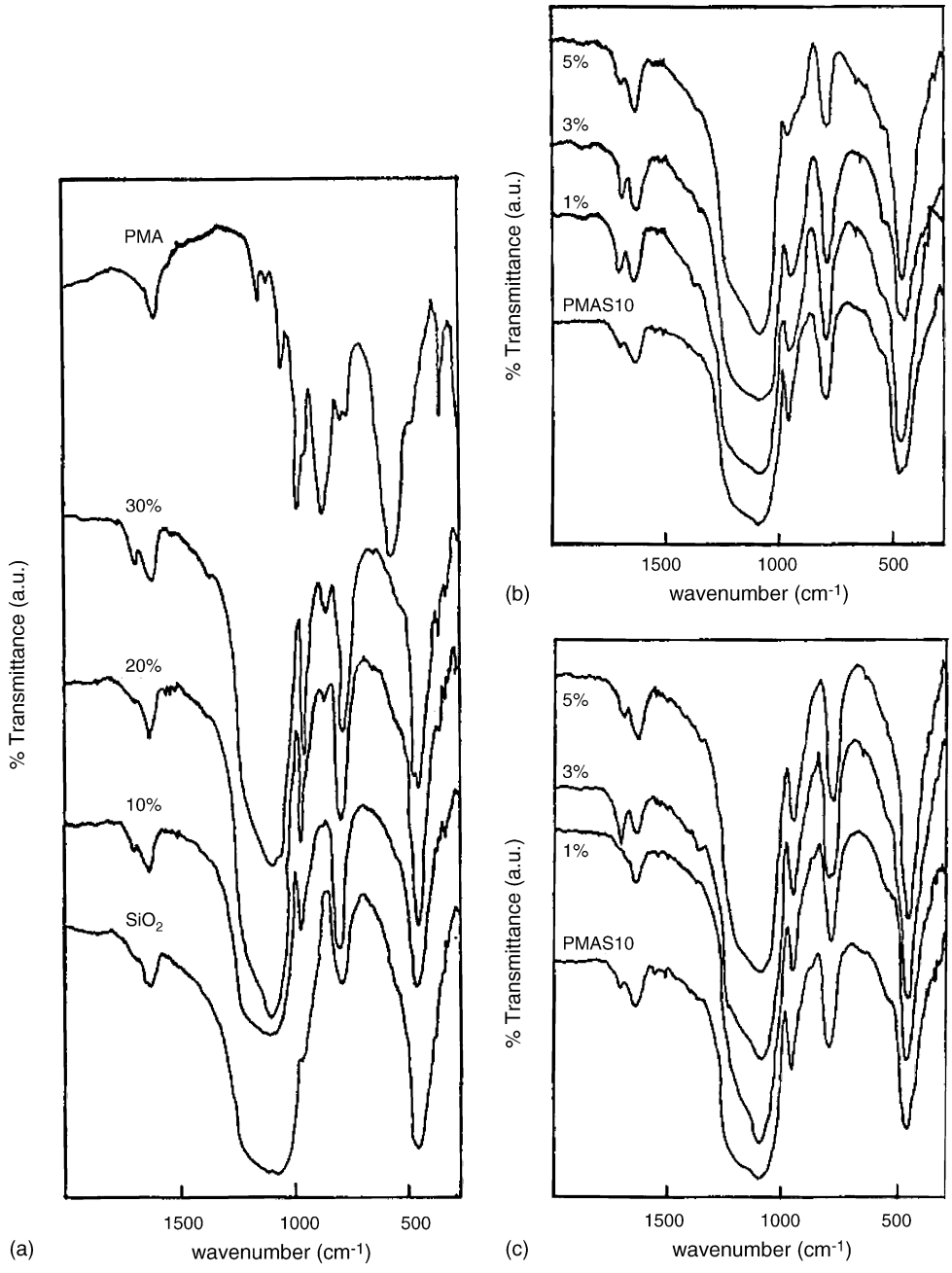

Fig. 2. (a) FT-IR spectra of pure SiO_2, pure PMA and PMA supported on silica and calcined at 350 °C for 4 h. (b) FT-IR spectra of PMAS10 catalyst doped with 1, 3 or 5 wt% Li^+ ions calcined at 350 °C for 4 h. (c) FT-IR spectra of PMAS10 catalyst doped with 1, 3 or 5 wt% Na^+ ions calcined at 350 °C for 4 h. (d) FT-IR spectra of PMAS10 catalyst doped with 1, 3 or 5 wt% K^+ ions calcined at 350 °C for 4 h.

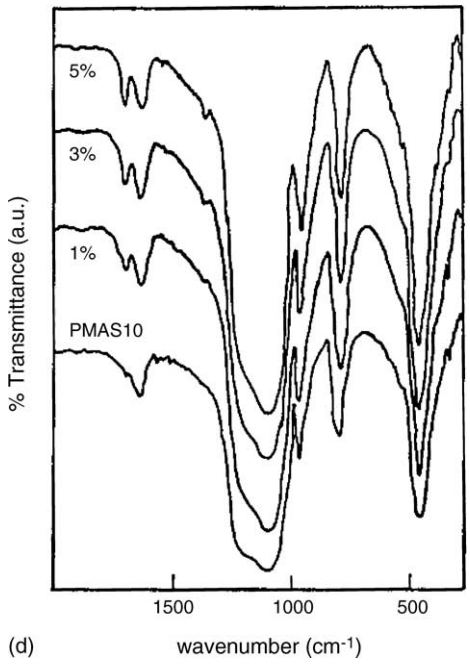

Fig. 2. (*Continued*).

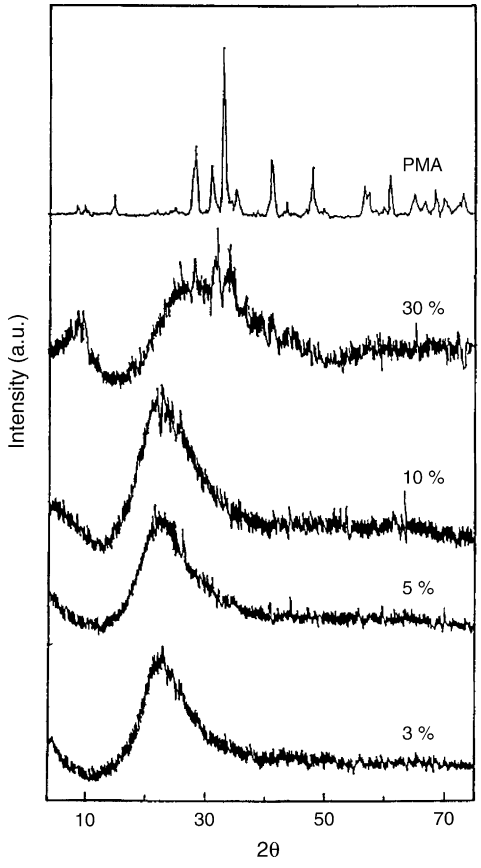

Fig. 3. XRD of pure PMA catalyst and supported on silica calcined at 350 °C for 4 h.

size data calculated from these measurements are shown in Table 1.

Table 1 shows that the tested samples suffered a continuous decrease in S_{BET} and total pore volume accompanied the increase in PMA loading. In contrast, the samples containing 20 or 30 wt% show a remarkable decrease of surface areas. In addition, the total pore volume also decreases while an increase in the average pore diameter is associated with the increase in PMA loading. The decrease in S_{BET} can be explained by the different distribution of PMA on SiO_2 surface. Also, these changes are suspected to be caused by plugging of support pores due to agglomeration of PMA. The pore size analysis for the tested samples showed a single peak distribution that is effectively located at the average pore radius as seen in Table 1, indicating a mesoporous structure is presented.

3.5. Determination of the surface acidic and basic sites

The catalytic dehydration–dehydrogenation of IPA over PMA supported on SiO_2 are shown in Fig. 4. The results show that the reaction products of IPA were propylene (major) and acetone (minor). However, the IPA dehydration has been used by several authors [36,37] as a test reaction for determining the acidity of different catalysts and it proceeds quickly on weak acidic sites [36]. Thus, it can be observed from Fig. 4 that the value of propylene yield on pure silica gel is rather simple reflecting the fact that only a small number of weak

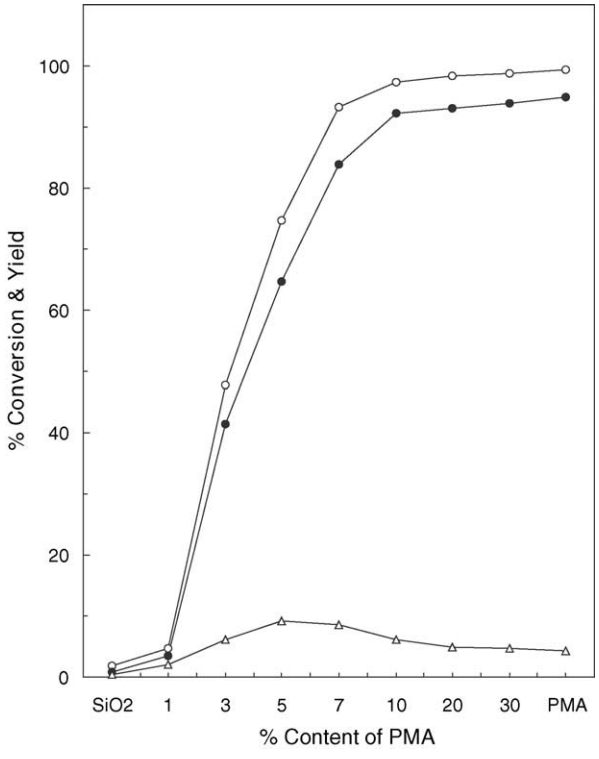

Fig. 4. Variation of % conversion of IPA (◯) and % yields of propylene (●) and acetone (△) with % content of PMA for the samples calcined at 350 °C.

Table 1
Textural properties of PMA supported on silica

PMA (wt%)	S_{BET} (m^2/g)	C-BET	Total pore volume (cm^3/g)	Average pore diameter (Å)
SiO_2	313.3	344.6	0.4055	322.6
1	310.9	307.5	0.3983	330.3
3	296.2	254.3	0.3883	339.8
5	288.0	391.3	0.3713	441.6
10	268.3	299.5	0.3432	348.7
20	225.9	383.2	0.2852	355.1
30	189.3	685.5	0.2256	367.5

acid sites exist on the surface of the support. Eventually, the addition of PMA into silica, the dehydration reaction sharply increases up to the addition of 10 wt% followed by a gradual increase up to 30 wt%. On the other hand, the dehydrogenation reaction as given by the % yield of acetone indicates that its value does not exceed more than 10%. In order to confirm the above observation, the relation between % conversion and % yield of propylene is shown in Fig. 5. It is revealed that, the % yield of propylene is found to increase linearly with % conversion. This means that the number of the acid sites, which were responsible for propylene yield, increases linearly with the increasing of the % loading of PMA. It is reasonable to mention here from the above results that the catalyst containing 10 wt% PMA has the capacity of acid sites enough to proceed the dehydration pathway of IPA nearly equal to that of unsupported PMA.

It is known that the chemisorption of pyridine was used as a probe base molecules to determine the acidity of the catalysts. It was reported that PY is selectively adsorbed on both Brönsted and Lewis acid sites [38,39]. Fig. 6 represents the effect of PY additions on the distribution of the reaction products of IPA over PMAS10 catalyst. These results show a continuous decrease in both conversion and propylene yield whereas a slight decrease in acetone yield was observed. The above results confirm that PMAS10 catalyst unpoisoned completely by the addition of PY and about 50% of the overall activity remains active towards the dehydration reaction as can be seen in Fig. 6. This means that PY can be chemisorbed on strong acid sites whereas the dehydration reaction of IPA proceeds on weak acid sites [39]. Thus, we can suggest that two acid sites exist on the catalyst surface, one is strong or intermediate and the second one is weak. The adsorption of pyridine bound to Lewis and Brönsted acid sites was monitored by FT-IR spectroscopy. Fig. 7 shows two spectra due to pyridine adsorbed on the pure SiO_2 and PMAS10 samples. The spectrum of PMAS10 shows two new bands assigned at around 1450 and 1540 cm^{-1} that are the characteristic bands of adsorbed pyridine [6]. On the other hand, the spectrum of pure SiO_2 revealed that negligible pyridine was adsorbed on pure silica. However, in accordance with the above results, the chemisorption of PY was also studied by TG technique and the results are shown in Fig. 8. The TG analysis shows that the sample exhibits weight loss on heating up

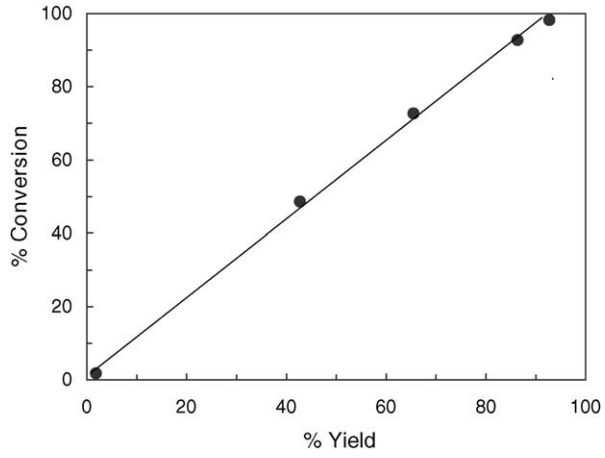

Fig. 5. Variation of % conversion of IPA with % yield of propylene for different ratios of PMA supported on SiO_2.

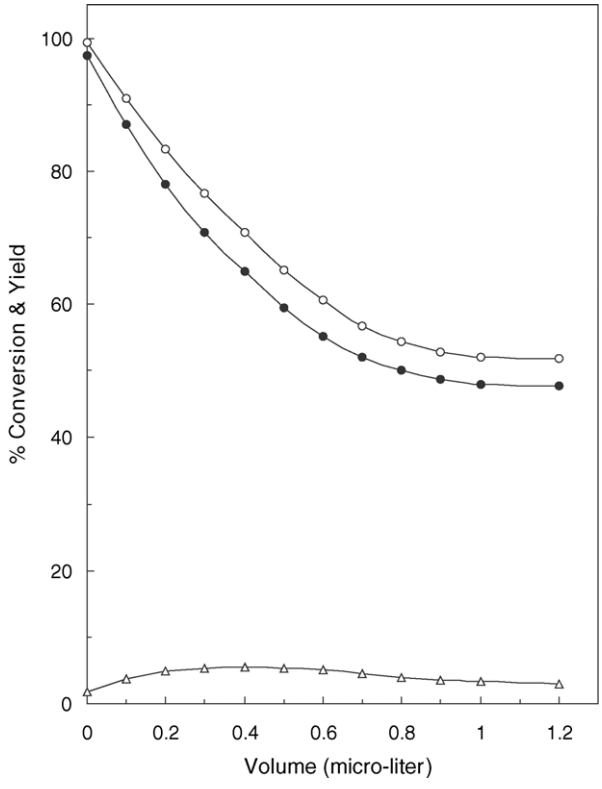

Fig. 6. Variation of % conversion of IPA (○) and % yields of propylene (●) and acetone (△) with the volume of pyridine for PMAS10 calcined at 350 °C.

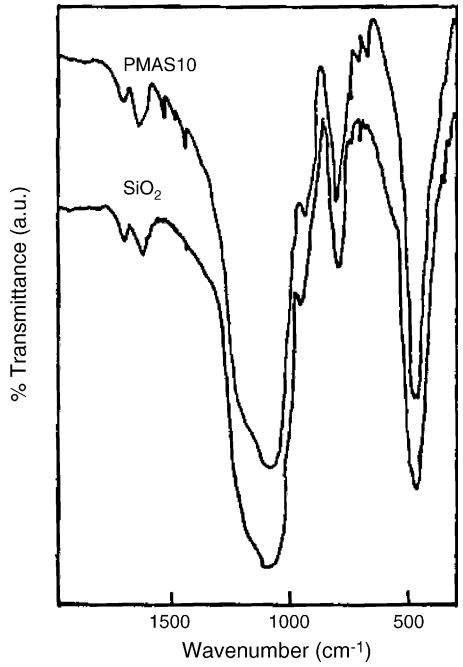

Fig. 7. FT-IR spectra of pyridine adsorption for pure SiO_2 and PMAS10 calcined at 350 °C.

to 350 °C. The weight loss observed below 200 °C may correspond to the desorption of weakly held physisorbed water and PY adsorbed on weak acid sites. Moreover, the weight loss above 200 °C reflects the desorption of PY chemisorbed on intermediate and/or strong strengths acid sites. From TG results and according to the reported method [20] for calculating the density of the acid sites, tested samples expose 6.0×10^{20}, 8.1×10^{20} and 6.8×10^{20} mmol acid sites per gm for SiO_2, PMAS10 and pure PMA catalysts, respectively. This reveals that the number of acid sites available on the surface of PMAS10 to PY adsorption is greater than that of unsupported PMA.

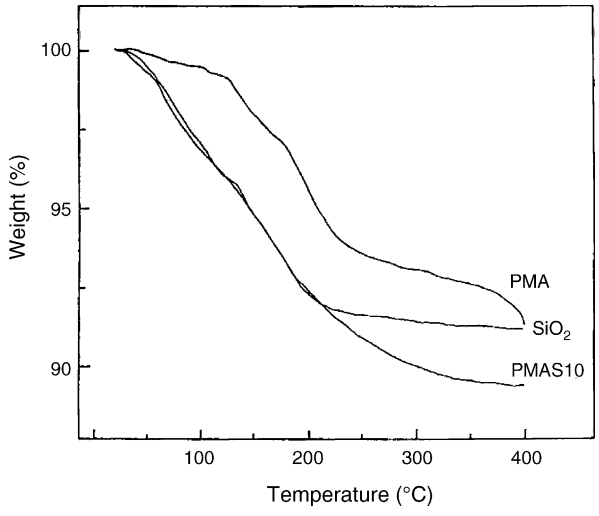

Fig. 8. TGA curves of SiO_2, PMA and PMAS10 after adsorption of pyridine.

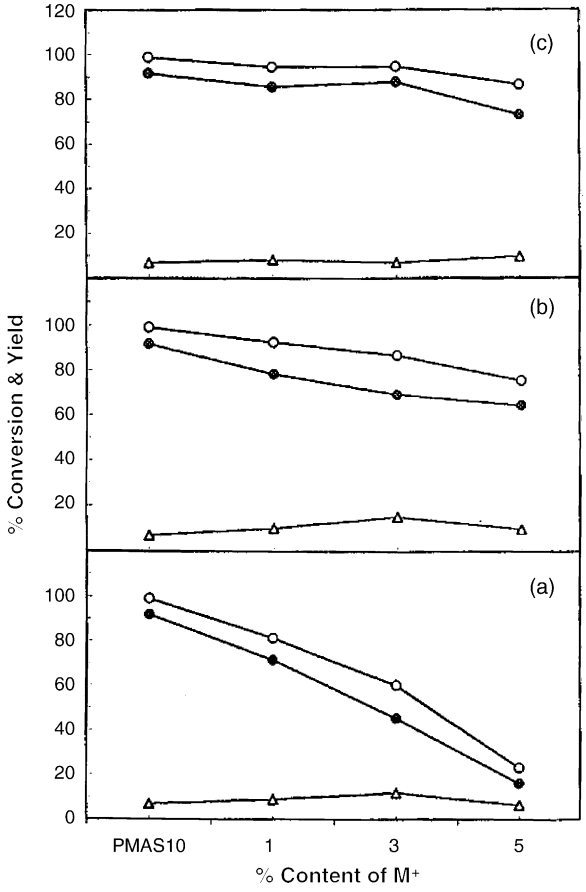

Fig. 9. Variation of % conversion of IPA (◯) and % yield of propylene (●) and aceton (△) with % content of (a) Li^+, (b) Na^+ and (c) K^+ ions, samples calcined at 350 °C for 4 h.

However, one way to control the acid site properties of HPA is through partial neutralization of the protons. This can be achieved by exchanging the acid form with a suitable metal ion (i.e. an alkali or alkaline earth salts). In this way, it is possible to reduce the number of protons in the compounds. Thus, Fig. 9 shows that the addition of small amounts of alkali metal hydroxides into PMAS10 catalyst reduces the yield of propylene reflecting an effective decrease in the concentration of acid sites. This decrease was found to follow the sequence,

$$\text{LiOH} \gg \text{NaOH} > \text{KOH}.$$

It is interesting to mention here from the above results that LiOH dopant sharply reduces the yield of propylene on increasing its content up to 5 wt% while Na and K hydroxide dopants do not exhibit the same behavior. According to the results of XRD, FT-IR spectra and that of recent work [2], a strong interaction between PMA and SiO_2, i.e. PMA highly dispersed in the pore structure of SiO_2, was observed. Moreover, Li^+ ion has an ionic radius small enough to occupy lattice position in SiO_2. Therefore, the observable reduction of the acid sites of PMAS10 catalyst (Fig. 9a) may be due to the replacement of protons of PMA by Li^+ ions in the bulk of SiO_2. In the accordance with this observation, the calcined samples gave a greenish colour except the samples doped

with Li^+ ions gave a white colour. This reflects again that a strong interaction between Li^+ ions and PMA.

3.6. Catalytic activity

The catalytic esterification of acetic acid with ethyl alcohol over silica supported PMA and PMAS10 doped with alkali metal hydroxides precalcined at 350 °C for 4 h was carried out at 225 °C and the results are shown in Figs. 10 and 11. Fig. 10 shows that pure SiO_2 support posses low activity and selectivity towards ethyl acetate formation. In addition, a significant increase in the yield of ethyl acetate was observed on SiO_2 supported PMA reaching a maximum value (≃65%) on the addition of 10 wt%, then gradually decreases up to the addition of 30 wt%. On the other hand, Fig. 11 shows that PMAS10 catalyst doped with Na or K-hydroxides led to further increase in the yield of ethyl acetate which reaches 75% on addition of 1 wt% Na or 3 wt% K hydroxides. The increase in their contents up to 5 wt% led to an observable decrease in both conversion and yield of ethyl acetate. Moreover, doping of PMAS10 catalyst with LiOH led to a continuous decrease in both conversion and yield of ethyl acetate up to the addition of 5 wt%.

However, the activity and selectivity of the prepared catalysts towards the formation of ethyl acetate, according to the above obtained results, depend on the acid sites distribution available on the catalyst surfaces. It was reported that the Brönsted acid sites of SiO_2 come from their surface hydroxyl groups [40]. These sites are active towards the formation of ester as indicated in Fig. 10, whereas they were inactive towards the formation of propylene (Fig. 4). Moreover, it was stated that Si-OH groups which must occurs in large amounts

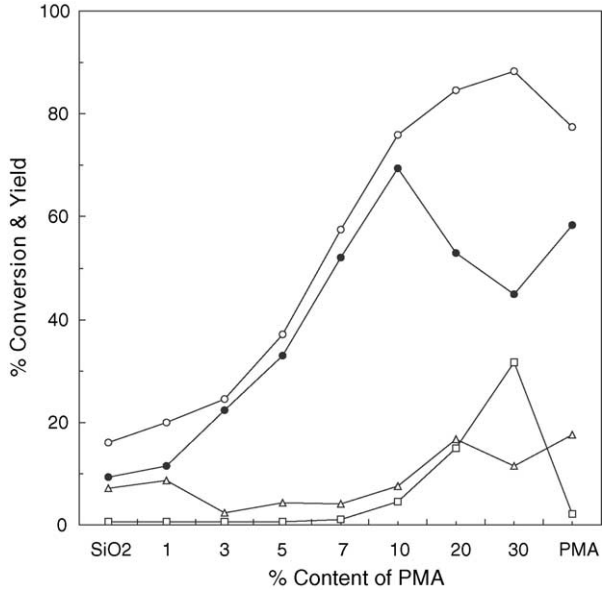

Fig. 10. Variation of % conversion of ethyl alcohol (◯) and % yields of ethyl acetate (●), ethylene (△) and acetaldehyde (□) with % content of PMA samples calcined at 350 °C for 4 h.

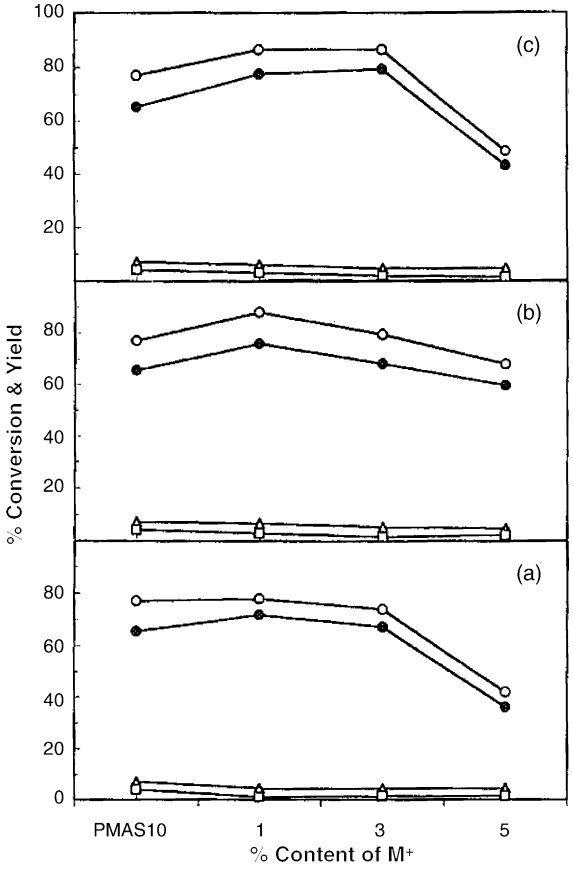

Fig. 11. Variation of % conversion of ethyl alcohol (◯) and % yields of ethyl acetate (●), ethylene (△) and acetaldehyde (□) of PMAS10 catalyst doped with (a) Li^+, (b) Na^+ and (c) K^+ ions, samples calcined at 350 °C for 4 h.

on SiO_2 surface are so strong [41]. Accordingly, we can suggest that the esterification reaction needs strong acid sites whereas the dehydration of IPA proceeds on weak acid sites [39]. Thus, the surface OH groups and surface oxygen ions [42] are responsible for the activity and selectivity of pure SiO_2. In addition, the hydroxyl groups can develop the acidic and basic properties, depending on the electronegativity and oxidation state of the metal site and on their coordination number with the surface [43]. Moreover, the presence of the Brönsted acid sites (proton) of PMA supported samples easily interact with adsorbed alcohol molecules. On the other hand, the presence of Lewis acid sites could be related to Mo^{5+} sites [44] produced during the reaction path. In addition, it has been stated that the terminal double bonded oxygens for molybdena are essential for creating Brönsted acid sites [45]. If attention is paid on the product selectivity (Fig. 10) it is clearly indicated that the intermediate or strong acid sites led to a direct dehydration products (i.e. ester) result on the supported catalysts in the range (1–10 wt%). A sharp decrease in the selectivity towards ester formation whereas an increase in the selectivity towards the byproducts, ethylene and acetaldehyde are noticed with the increasing of PMA up to 30 wt%. In order to confirm the above observation, Fig. 12 represents

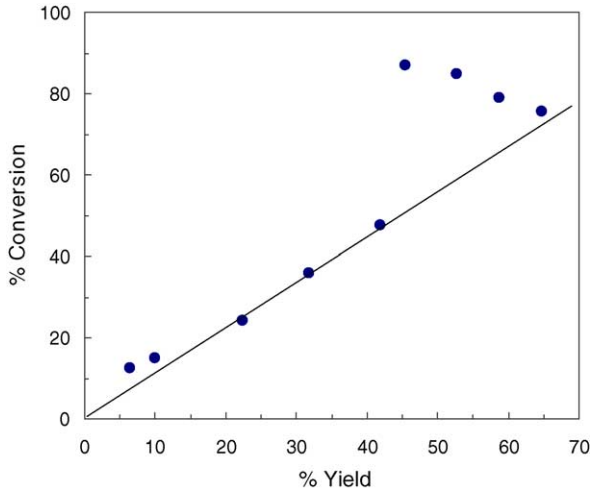

Fig. 12. Variation of % conversion of ethyl alcohol and % yield of ethyl acetate for different ratios of PMA supported on SiO_2.

the relation between the conversion and the yield of ethyl acetate for all supported catalysts. It shows that the relation is a linear correlation only for the samples containing PMA (1–10%) range. This trend suggests that the reaction proceeds via two contributions: one depends mainly on the surface acidity while the other does not. These results are in agreement with that observed in Fig. 10. The sharp decrease in the selectivity towards the formation of ester with the increase of PMA above 10 wt% reveals that the adding of Brönsted acid site (proton) is not suitable site for the production of ethyl acetate. In contrast with Brönsted acids, Lewis acids in catalyst support bring definitely different results.

It was reported that, PMA is multielectron oxidants [46], and the mechanism of reduction of Keggin unit involves the transfer of as many as six electrons to the unit without collapse of the structure. The mixed valences are characterized by an intense blue colour (which is observed after the reaction runs) are caused by inter valence transitions. Therefore, the generation of Lewis acid sites could be related to unsaturated Mo^{5+} sites produced during the reaction path [47]. Moreover, it is known that Lewis acid sites are electron deficient centers probably consisting of metal ions with particular high electron affinity, while alcohol molecules tend to be electron donors. Consequently, the observable increase in the yield of ethylene on the catalysts containing PMA > 10 wt% may attributed to presence of Lewis acid sites. Moreover, it supports the view of dependence of the activity and selectivity, besides the acidity of the catalysts, on the ability of the catalysts to activate and incorporate gaseous oxygen into crystal lattice oxygen (O^{2-}) by electron transfer from the metal oxide [46] simultaneously a release of electron (from alcohol) to the surface of the catalyst occurs:

$$\text{surface} \underset{O^{2-}}{\overset{2e}{\longleftrightarrow}} \text{oxygen in the gas phase.}$$

Thus, the dehydrogenation step is rather easy because both electrophilic and nucleophilic oxygen species can abstract hydrogen.

In the acid catalyzed reactions over solid catalysts, the control of acidity (strength and amount) is important, because each reaction requires proper acidity to proceed selectively. Consequently and according to the results of acidity, the catalytic behavior of alkali doped PMAS10 can be interpreted in terms of the modification of the acid sites distribution. It is of interest to notice from the results included in this work that the addition of Li^+ ions into PMAS10 (Fig. 9) decreases its acidic sites. On the other hand, the relation between % selectivity and % doping (not shown) indicated that the selectivity to ester formation and its value unchanged with increasing the doping up to 5 wt%. This means that the acid sites responsible for the ester formation were slight affected by the addition of LiOH. On the other hand, according to the dehydration of IPA, it was concluded that the acidity determined was corresponded to the weak acid sites. These weak acid sites were destroyed by the addition of lithium hydroxide, as shown in Fig. 9. Moreover, it was observed that from the FT-IR results that the addition of LiOH into PMAS10 increases the intensity of the band corresponded to OH groups. Consequently, we can suggest that the incorporation of Li^+ ions may destroy the weak Brönsted acid sites (protons of PMA) whereas it increases the Brönsted (proton donar OH's) acid sites.

However, as a matter of fact, it has been shown that the effect of alkali cations on the catalytic activity and selectivity of PMA was explained in terms of electronegativity (via electrostatic effects of these cations on the strength of the molybdenum–oxygen bond) and Brönsted acidity [47,48]. Also, the decrease of electronegativity of the alkali cations was reported to be inversely proportional to the activity of the alkali metal salts of PMA [47]. Moreover, the ionic radii of Na^+ or K^+ cations are greater than that of Li^+ ions which they are difficult to diffuse in the lattice network of SiO_2 even in the top surface layers. Thus, the presence of basic sites adjacent to acidic sites on the surface of the catalyst may enhance the dehydration reaction, this view has been supported by Bakashi and Gavalus [49].

4. Conclusions

From the results presented and discussed above, it can be concluded that:

(1) Characterization of supported catalysts by TG, DTA, IR and XRD suggests a strong interaction between the host silica network and the guest PMA molecules.
(2) PMA loaded on SiO_2 acts as active and selective catalysts towards the formation of ethyl acetate. The maximum yield of ester (≃65%) with low amount of side reaction was obtained on the catalyst containing 10 wt% PMA. In fact, this result was found better than that of unsupported acid. Moreover, the yield of ethyl acetate was modified

(≃75%) on the addition of 1 or 3 wt% Na or K hydroxides.

(3) The acidity measurements revealed that two acid sites exist on the catalyst surfaces, one was weak and the other was intermediate or strong. The dehydration reaction towards ethyl acetate selectively proceeded on the strong Brönsted acid sites.

(4) In the gas-phase esterification reaction over PMA supported on high surface area SiO_2, the protons are not only playing the main role for ethyl acetate formation but the presence of the terminal double bonded oxygens for molybdena and OH groups also playing a role as Brönsted acid sites in the ester formation.

References

[1] Y. Izumi, K. Hisano, T. Hida, J. Appl. Catal. 181 (1999) 277.
[2] A. Molnar, C. Keresszegi, B. Torok, J. Appl. Catal. A 189 (1999) 217.
[3] C. Marchal-Roch, N. Laronze, R. Villanneau, N. Guillou, A. Teze, G. Herve, J. Catal. 190 (2000) 173.
[4] W. Kuang, A. Rives, M. Fournier, R. Hubaut, J. Appl. Catal. A 250 (2003) 221.
[5] W. Chu, Z. Zhao, W. Sun, X. Ye, Y. Wa, Catal. Lett. 55 (1998) 57.
[6] A. Kukovecz, Zs. Balogi, Z. Konya, M. Toba, P. Lentz, S.-I. Niwa, F. Mizukami, A. Molnar, J.B. Nagy, I. Kiricsi, J. Appl. Catal. A 228 (2002) 83.
[7] T. Okuhara, N. Mizuno, M. Misona, Adv. Catal. 41 (1996) 113.
[8] A. Kukovecz, Z. Konya, I. Kiricsi, J. Mol. Struct. 565–566 (2001) 121.
[9] P. Trens, J.W. Peckett, V.N. Stathopoutos, M.J. Hudson, P.J. Pomonis, J. Appl. Catal. A 241 (2003) 217.
[10] T.O. Kuhara, C. Hu, M. Mashimoto, M. Misono, Bull. Chem. Soc. Jpn. 67 (1994) 1186.
[11] Y. Wu, X. Ye, X. Yang, X. Wang, W. Chu, Y. Hu, Ind. Eng. Chem. Res. 35 (1996) 2546.
[12] T. Okuhara, T. Nishimura, H. Watanabe, M. Misono, J. Mol. Catal. 74 (1992) 247.
[13] T. Okuhara, T. Nishimura, K. Ohashi, M. Misono, Chem. Lett. 120 (1990).
[14] K. Segawa, N. Kihara, H. Yamamoto, J. Mol. Catal. 74 (1992) 213.
[15] Y. Izumi, M. Ono, M. Kitagawa, M. Yoshida, K. Urabe, Microporous Mater. 5 (1995) 255.
[16] Y. Izumi, K. Urabe, M. Onaka, Microporous Mesoporous Mater. 21 (1998) 227.
[17] A.A. Said, J. Chem. Technol. Biotechnol. 78 (2003) 733.
[18] A.A. Said, M.M.M. Abd El-Wahab, G.A. El-Shobaky, Oxid. Commun. 1 (2004) 27.
[19] M.M.M. Abd El-Wahab, A.A. Said, Sh. S. El-Shihry, Monatshefte fur chemie 135 (2004) 357.
[20] M.A. Makarova, E.A. Paukshtis, J.M. Thomas, C. Williams, K.I. Zamaraev, J. Catal. 149 (1994) 36.
[21] C.T. Fishel, R.J. Davis, Catal. Lett. 25 (1994) 87.
[22] M. Misono, V. Mizuno, K. Katamura, A. Kasai, K. Sakata, T. Okuhara, Y. Yaneda, Bull. Chem. Soc. Jpn. 55 (1982) 400.
[23] D. Farcasiu, T.Q. Li, J. Catal. 152 (1995) 192.
[24] C.R. Deltcheff, M. Amirouche, M. Fournier, J. Catal. 138 (1992) 445.
[25] R.A. Nyquist, R.O. Kegel, Infrared Spectra of Inorganic Compounds, Academic Press, New York/London, 1971.
[26] T. Tanaka, Y. Nishimura, S. Kawasaki, M. Ono, T. Funabiki, S. Yoshida, J. Catal. 118 (1989) 327.
[27] A. Coroma, Chem. Rev. 95 (1995) 559.
[28] I. Kawafun, G. Matsubayashi, Bull. Chem. Soc. Jpn. 68 (1995) 838.
[29] N. Mizuno, M. Tateishi, M. Iwamoto, J. Appl. Catal. A 128 (1995) 165.
[30] J. Ponzniczek, A. Bielanski, I. Kulszewicz-Bojer, M. Zagorska, K. Kruczala, K. Dyrek, A. Pron, J. Mol. Catal. 69 (1991) 223.
[31] C. Rocchiccioli-Deltecheff, M. Fournier, R. Franck, R. Thouvenot, Inorg. Chem. 22 (1983) 207.
[32] I.V. Kozhevnikov, K.R. Kloerstra, A. Sinnema, H.W. Zandbergen, H. Van Bekkum, J. Mol. Catal. A Chem. 114 (1996) 287.
[33] Y. Izumi, M. Ono, M. Kitagawa, M. Yoshida, K. Urabe, Microporous Mater. 5 (1995) 255.
[34] Y. Izumi, K. Urabe, M. Onaka, Microporous Mesoporous Mater. 21 (1998) 227.
[35] S. Brunauer, L.S. Deming, W.S. Deming, E. Teller, J. Am. Chem. Soc. 62 (1940) 1723.
[36] J.R. Sohn, H.J. Jang, J. Mol. Catal. 64 (1991) 349.
[37] L. Vardonis, P.G. Koutsoukos, A. Lycourghiotis, J. Catal. 98 (1986) 296;
L. Vardonis, P.G. Koutsoukos, A. Lycourghiotis, Colloids Surf. 50 (1990) 353.
[38] M. Ziolek, J. Kujawa, O. Saur, A. Aboulyat, J.C. Lavalley, J. Mol. Catal. A 112 (1996) 125.
[39] M.A. Aramendia, V. Borau, C. Jimenez, J.M. Marinas, A. Porras, F.J. Urbano, J. Catal. 161 (1996) 829.
[40] Y. Wang, W. Li, React. Kinet. Catal. Lett. 69 (2000) 169.
[41] H.P. Bohm, Adv. Catal. 16 (1969) 179.
[42] H. Knzinger, H. Buhl, K. Kochlofl, J. Catal. 24 (1972) 57.
[43] T. Seiyama, Metal Oxides and Their Catalytic Action, Kodansha, Tokyo, 1978.
[44] C. Martin, I. Martin, C. del Moral, V. Rives, J. Catal. 146 (1994) 415.
[45] T. Kataoka, J.A. Dumesic, J. Catal. 112 (1988) 66.
[46] M. Ai, J. Catal. 60 (1979) 306.
[47] M. Akimoto, Y. Tsuchida, K. Sato, E. Echigoya, J. Catal. 72 (1981) 83.
[48] M. Akimoto, K. Shima, E. Echigoya, J. Chem. Soc. Faraday Trans. 1 79 (1983) 2467.
[49] K.R. Bakashi, G.R. Gavalas, J. Catal. 32 (1975) 312.